

# Lawrence Berkeley National Laboratory

## Recent Work

### Title

THE VALENCE BAND STRUCTURE OF SILVER ALONG A FROM ANGLE-RESOLVED PHOTOEMISSION

### Permalink

<https://escholarship.org/uc/item/09635999>

### Author

Wehner, P.S.

### Publication Date

1978-08-01

Submitted to Physical Review B

LBL-8218  
Preprint c.2

THE VALENCE BAND STRUCTURE OF SILVER  
ALONG  $\Lambda$  FROM ANGLE-RESOLVED PHOTOEMISSION

P. S. Wehner, R. S. Williams, S. D. Kevan,  
D. Denley, and D. A. Shirley

September 1978

RECEIVED  
PHYSICS  
LABORATORY

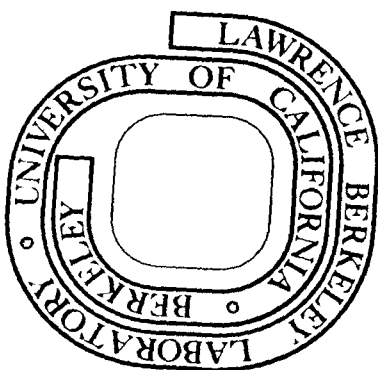
DEC 22 1978

LIBRARY AND  
DOCUMENTS SECTION

Prepared for the U. S. Department of Energy  
under Contract W-7405-ENG-48

TWO-WEEK LOAN COPY

This is a Library Circulating Copy  
which may be borrowed for two weeks.  
For a personal retention copy, call  
Tech. Info. Division, Ext. 6782



LBL-8218  
c.2

## **DISCLAIMER**

This document was prepared as an account of work sponsored by the United States Government. While this document is believed to contain correct information, neither the United States Government nor any agency thereof, nor the Regents of the University of California, nor any of their employees, makes any warranty, express or implied, or assumes any legal responsibility for the accuracy, completeness, or usefulness of any information, apparatus, product, or process disclosed, or represents that its use would not infringe privately owned rights. Reference herein to any specific commercial product, process, or service by its trade name, trademark, manufacturer, or otherwise, does not necessarily constitute or imply its endorsement, recommendation, or favoring by the United States Government or any agency thereof, or the Regents of the University of California. The views and opinions of authors expressed herein do not necessarily state or reflect those of the United States Government or any agency thereof or the Regents of the University of California.

THE VALENCE BAND STRUCTURE OF SILVER  
ALONG  $\Lambda$  FROM ANGLE-RESOLVED PHOTOEMISSIONP. S. Wehner,<sup>\*</sup> R. S. Williams,<sup>†</sup> S. D. Kevan,  
D. Denley,<sup>‡</sup> and D. A. ShirleyMaterials and Molecular Research Division  
Lawrence Berkeley Laboratory  
and  
Department of Chemistry  
University of California  
Berkeley, California 94720

September 1978

## ABSTRACT

Angle-resolved normal photoemission spectra of Ag(111) are reported for photon energies  $h\nu = 6-32$  eV, obtained by the use of synchrotron radiation. Very good agreement was found with the theoretical RAPW band structure of Christensen. Experimental dispersion relations along  $\Lambda$  were derived and tabulated. The d-band spacings at  $\Gamma$  were determined for the first time and were interpreted to yield the "ligand field" parameters  $10Dq = 0.865 \pm 0.027$  eV,  $\xi(4d) = 0.232 \pm 0.011$  eV. These parameters, which are meaningful only at  $\Gamma$ , are in excellent agreement with Christensen's band structure. The spin-orbit parameter is very close to the free-atom value, and the positive sign of  $10Dq$  indicates attractive interaction of the electrons with neighbor ion cores. Two pieces of evidence for indirect transitions via thermal broadening were noted. A resonance at  $h\nu = 22$  eV in the band-4 ( $\Gamma_7$ ) intensity was attributed to a flat region in band 7

<sup>\*</sup>Present address: Tennessee Eastman Co., Kingsport, TN 37662.

<sup>†</sup>Present address: Bell Laboratories, Murray Hill, NJ 07974.

<sup>‡</sup>Also with the Department of Physics, University of California, Berkeley.

( $\Gamma_6$ ). The flatness in band 7 (and perhaps band 8) also yields a new effect equivalent to the angle-resolved secondary electron emission (ARSEE) phenomenon of Willis and co-workers. In this case electrons moving in the [111] direction are scattered down into band 7 and trapped, yielding a peak at 17 eV kinetic energy.

## I. INTRODUCTION

Silver occupies an interesting position among transition- and noble metals because its 4d bands are relatively narrow (3 eV bandwidth), and they lie well (4 eV) below the Fermi energy. In addition, the spin-orbit coupling strength of  $\xi(4d) = 0.22$  eV in the free atom is comparable to the crystal potential. In fact, early x-ray photoemission (XPS) spectra<sup>1,2</sup> in silver showed a d-band density of states that somewhat resembled a spin-orbit doublet, perturbed by crystal-field splitting. Analysis<sup>2,3</sup> showed that this picture was not viable, however; and later, higher-resolution XPS studies yielded additional features that require a band-structure interpretation.<sup>4,5</sup> We shall return below to a comparison of the spin-orbit coupling strength with the crystal-field energy in the context of 4d-band splitting at the  $\Gamma$  point in the Brillouin Zone.

Ultraviolet photoemission studies of silver have been carried out under a variety of conditions.<sup>6-14</sup> The major conclusion of these studies is that angle-resolved photoemission (ARP) spectra from single crystals can be interpreted, using the direct-transition model, to yield results in good agreement with predictions based on the theoretical dispersion relations of the valence bands of silver. Hansson and Flodström,<sup>13</sup> in particular, gave very detailed evidence for this conclusion on the basis of their ARP studies at photon energies in the range 7.0 - 11.6 eV. These workers found nearly quantitative agreement between their experimental peak positions and predictions based on Christensen's relativistic band structure,<sup>15</sup> coupled

with the direct-transition model. Liebowitz and Shevchik<sup>14</sup> drew similar conclusions from ARP spectra obtained using rare-gas lamps at five energies between 11.6 eV and 40.8 eV.

Encouraged by these results, as well as by our own earlier ARP studies of copper, in which the direct-transition model was found to apply for photon energies in the range 32-160 eV,<sup>16</sup> we have carried out ARP studies of the (111) face of silver in normal emission over the energy range 6-32 eV, using synchrotron radiation. By extending the photon energy range up to 32 eV we were able to study the valence-band dispersion relation along the  $\Lambda$  symmetry direction to the  $\Gamma$  point. In particular, the d-band energies at  $\Gamma$  were determined for the first time. These higher photon energies also allowed us to probe the total valence bands; for photon energies  $h\nu \geq 16$  eV all the valence bands were energetically accessible.

Two particularly interesting observations were made during the course of this research. A sharp resonance in the intensity of a peak arising from the  $\Gamma_7$  band was observed at  $h\nu = 22$  eV, enabling us to locate the energy of this band at a  $\vec{k}$  point near  $\Gamma$ . In addition, an interesting final-state effect was observed. For  $h\nu \geq 26$  eV, photoemitted electrons are trapped in a high-energy band (or bands) with a high density of states near  $\Gamma$ , which they apparently reach through scattering processes. From this state in the crystal they emerge in the normal direction at a fixed kinetic energy of 17 eV.

Experimental procedures are described in Section II. Dispersion relations along  $\Lambda$  are derived and presented in Section III, and the energies of the d bands at  $\Gamma$  are discussed. Section IV is devoted to the band 4 to band 7 resonance at  $h\nu = 22$  eV, and the 17-eV kinetic energy feature that appears in the spectrum for  $h\nu > 26$  eV. A summary is given in Section V.

## II. EXPERIMENTAL

A high-purity single crystal of silver was cut to produce a (111) surface orientation and polished to 1-micron smoothness. It was etched repeatedly in a solution of concentrated nitric acid saturated with silver nitrate to remove the damage layer. Back-reflection Laue photographs were taken to check the post-treatment crystalline orientation. They showed it to be correct to within  $1^\circ$  or better. Sharp diffraction features appeared in the patterns, indicating the absence of a deep damage layer. After final insertion into the ultrahigh vacuum chamber, the crystal was further cleaned in situ by repeated cycles of argon-ion bombardment and annealing at  $600^\circ\text{K}$ . Auger analysis showed no remaining surface contaminants: the limit of detectability was 0.03 monolayers.

The photoemission measurements were performed on the  $8^\circ$  branch line of Beam Line I at the Stanford Synchrotron Radiation Laboratory, using an experimental chamber which has been described in full detail elsewhere.<sup>17,18</sup> The electric field vector of the highly-polarized ( $\geq 97\%$ ) incident radiation lay in the



horizontal plane defined by the Poynting vector of the radiation and the propagation direction of the detected photoelectrons; the angle between the latter two was fixed at  $145^\circ$ . Only electrons emitted in a cone of  $5^\circ$  half-angle around the surface normal of the sample were collected. The total energy resolution (monochromator plus electron energy analyzer) was ca. 0.26 eV.

Photoemission spectra were taken normal to the (111) plane throughout the available photon energy range  $h\nu = 6-32$  eV. Counting rates were excellent ( $\sim 10^4 \text{ sec}^{-1}$ ) and a spectrum could be taken with good statistics in 5 minutes. Figure 1 shows the spectra.

### III. VALENCE-BAND DISPERSION RELATIONS

To interpret the spectra shown in Fig. 1, it is necessary to establish a theoretical model that can explain at least the principal spectral features. That the direct-transition model is adequate for similar spectra has already been well established,<sup>13,14,16</sup> and we need not belabor it further here. Rather, we shall discuss briefly the qualifications that must be made before a direct-transition model interpretation can be applied, then proceed to derive band-structure information for silver along the  $\Lambda$  line. We note that until now it has been common practice in angle-resolved photoemission spectroscopy of metals to plot theoretical dispersion relations along symmetry lines (or elsewhere in the Brillouin Zone), superimpose experimental points, and draw conclusions about the extent of the agreement

with the direct-transition model, assuming the correctness of the theoretical band structure (e.g., Refs. 13, 14, 16). Now that the model is well established, it is becoming generally worthwhile to go a step further and construct experimental dispersion relations (to the extent that this is possible), presenting results in tabular rather than only in graphical form. Of course, this approach is fraught with obvious pitfalls (e.g., some of the BZ or even of the  $\Lambda$  line is inaccessible, some transitions are unresolved or unobserved, theoretical final-state bands must be used to derive initial-state dispersion relations, many-body effects are neglected, etc.). Nevertheless we shall make such an analysis below, mostly using our own spectra but also taking into account other relevant data.<sup>12-14</sup>

First let us discuss which features of the spectra arise from direct transitions. It is the nature of photoemission from solids that several mechanisms usually contribute to the spectral intensity. In the case of Ag[111] photoemission we believe that all the spectral features are at least qualitatively understood. Starting down from the Fermi energy,  $E_F$ , a surface-state peak appears at  $0.13 \pm 0.05$  eV binding energy. This state has been well characterized previously,<sup>12,13</sup> and need not be discussed further except to note that our spectra agree well with the earlier work when allowance is made for our lower angular- and energy-resolution. In particular, our 7 eV and 8 eV spectra are in essential agreement with the s- and p-polarized 7.8 eV spectra of Hansson and Flodström,<sup>13</sup>

when the latter are suitably weighted for our experimental geometry.

Proceeding to higher binding energy, and to the higher photon-energy spectra, the first 4 eV from  $E_F$  are dominated by a low-intensity, flat plateau of spectral intensity. This is familiar as the "s-p bands" in (angle-integrated) photoemission spectra from polycrystalline samples, and of course in the density of states.<sup>2</sup> In angle-resolved photoemission the source of this plateau is less obvious. It cannot arise from direct transitions from the s-p bands, which lead instead to a peak in the 0-4 eV binding-energy region that moves across this region as the photon energy is varied. This peak is clearly visible in the spectra for photon energies in the  $h\nu = 6 - 12$  eV range. The plateau must be attributed instead to indirect transitions, especially (and perhaps exclusively) phonon-assisted transitions. In fact there exists in our spectra a rather neat piece of evidence for this conclusion. Referring to Fig. 2, in which Christensen's<sup>15</sup> band structure for silver along  $\Lambda$  is shown, we note that the height of the plateau, and thus its intensity, decreases to a minimum at  $h\nu = 25$  eV, then increases again. This is the energy at which the  $\Gamma$  point is being sampled along the  $\Gamma L$  direction, and this point lies farthest from band 6, which goes up nearly to  $E_F$  and constitutes the s-p band plateau when the BZ is sampled along the  $\Lambda$  direction. Thermally-induced phonon-assisted transitions<sup>19</sup> may in fact achieve just this kind of sampling (see below). If we think of this

effect as leading to sampling of the BZ along  $\Lambda$  for a mean distance (in units of  $\pi/a$ ) which is determined by the phonon momentum, then the effect will clearly be minimal when the nominal sampling point is at  $\Gamma$ , and the intensity minimum in the plateau will fall at  $h\nu = 25$  eV, as observed. We note that the sixth valence band rises toward  $E_F$  as we move from  $\Gamma$  toward the Brillouin Zone boundary in most directions in the Zone. Therefore the above argument will apply equally well if phonon-assisted transitions result in a three-dimensional sampling of the zone. We shall return below to other evidence for this effect in connection with certain features of the very high resolution spectra presented by Roloff and Neddermeyer.<sup>12</sup>

The remaining features of these spectra are the direct-transition peaks, discussed below, the 17-eV kinetic energy peak, discussed in Section IV, and the inelastic tails in the electron distribution. About this tail we simply note that electrons can be scattered both in the sample and in the spectrometer, so that precise comparisons of data from different sources may show different intensities in this feature.

Peak positions derived from our spectra are shown as open circles in Fig. 2. In deriving the  $(\vec{k}, E)$  coordinates of these data, we used the following procedure:

1. On the basis of the direct-transition model, the final states were found to lie in the second BZ along the [111] direction, for all the photon energies that

were used. Thus the reciprocal lattice vector  $\vec{G} = (1,1,1)$  connects the initial and final crystal momenta in the equation  $\vec{k}_f = \vec{k}_i + \vec{G}$ .

2. From Christensen's band structure, only one final-state band along the  $\Lambda$  line is available for photoemission throughout the entire lower portion of the photon energy range covered. This is the seventh band from the bottom, which has mostly  $\vec{G} = (1,1,1)$  character up to  $\sim 16$  eV, where it becomes strongly admixed and a gap develops. We ignored this gap. To derive final-state  $\vec{k}_f$  values at higher energies we extended this band using a free-electron dispersion relation.<sup>14,16</sup>

3. The above procedures yielded the  $\vec{k}_i$  coordinate, for projecting the crystal momentum back into the first BZ. Energy difference between initial and final states were given by the photon energies. Relative energies of valence bands were therefore determined quite accurately (to  $\pm 0.05$  eV) from relative peak positions. Careful monitoring of the analyzer voltages assured that the observed binding energies varied smoothly to within these limits as the photon energy was raised.

4. The Fermi energy was taken as the energy at half-height on the incline at the end of the "s-p band" plateau, for spectra in which this feature was clear: i.e., about two-thirds of our spectra. Reference

voltages were used to establish the Fermi energies of the other third. In the adjusted spectra the derived work functions showed an rms scatter of only  $\pm 0.03$  eV.

As Fig. 2 shows, our data yield smooth variations of  $E$  with  $\vec{k}$ , and they show generally very good agreement with Christensen's band structure. All six bands in fact yield data points somewhere along  $\Lambda$ , and there are no peaks in our spectra that yield points which do not correspond to a band along  $\Lambda$ . The valence bands were energetically inaccessible near  $L$ . Elsewhere in the BZ, band 1 did not appear near  $\Gamma$ , presumably because its s-like character near  $\Gamma$  leads to a low photoemission cross section. Band 3 was missing from most of our spectra. With these exceptions, all bands yielded peaks (or definite evidence for unresolved peaks) in nearly all spectra.

In addition to our Ag(111) spectra, taken at 17 photon energies, ARP spectra are also available taken with laboratory sources at some 11 distinct energies, from three other laboratories.<sup>12-14</sup> Peak positions derived from these other spectra on the direct transition model are shown as filled circles in Fig. 2. The relative peak positions in all the other 11 spectra were all in excellent agreement with ours, to the extent that comparisons could be made, when due account was taken of the somewhat higher resolution of Hansson and Flodström's data,<sup>13</sup> and of the very high resolution of the spectra of Roloff and Neddermeyer.<sup>12</sup> However, we found that the absolute binding

energies of the bands relative to  $E_F$  did not agree among the three sets of data as well as would be expected on the basis of their precision. The cause of this discrepancy may lie in the placement of the Fermi energy by the three groups, or it may arise from different methods used for locating peak binding energies. We note in this connection that the peak binding energies which we would derive from Fig. 3 of Ref. 13 are somewhat higher than those shown in their Fig. 13. At any rate a unique explanation of the binding-energy discrepancy has eluded us. For the purpose of this paper we have brought all the data very nicely into register by adding 0.18 eV to the binding energies given by Hansson and Flodström<sup>13</sup> in their Fig. 13, and subtracting 0.25 eV from the binding energies of the 21.22 eV and 16.85 eV spectra of Roloff and Neddermeyer.<sup>12</sup> The data, thus adjusted, were re-plotted in Fig. 3. The energy bands have been adjusted somewhat where the data warranted, to afford better agreement with experiment. With the exception of three points, all the experimental data are in satisfactory agreement with the adjusted bands; i.e., in most cases within 0.1 eV or less. The discrepancies were slightly larger for the lowest band and for the middle point from the 40.8 eV spectrum of Liebowitz, and Shevchik (at  $E_B = 6$  eV,  $|k| = 1.3$ ): in these two cases the experimental uncertainties in peak position were also larger.

In adjusting the bands the photoemission data did not extend to the L point, but fortunately the electron tunneling results

of Jaklevic and Lambe<sup>20</sup> could be used to tie down the position of the highest valence band (band 6) at  $E_F - 0.3$  eV.

The three data points that showed genuine disagreement with the direct transition model all lie near 4 eV binding energy, and each is derived from a small shoulder on the low- $E_B$  side of the main peak in the high-resolution spectra of Roloff and Neddermeyer,<sup>12</sup> at photon energies of 11.83 eV, 16.85 eV, and 21.22 eV, respectively. Although only in these spectra was the energy resolution high enough to resolve this weak feature, evidence for it (in the form of extra width near the foot of the main peak) can be found on careful inspection of the 11.6 eV spectrum of Ref. 13 and of our own spectra between 12 eV and 20 eV and at 30 eV photon energy. We interpret this small peak at 4 eV as arising from indirect transitions involving valence bands that rise up to  $\sim(E_F - 4$  eV) and become flat near the BZ boundary (e.g., near the X, K, and L points<sup>15</sup>). As in the case of the "s-p band" plateau, such transitions could be phonon-assisted, and they would in the limiting case yield a spectrum resembling the density of states.

We have derived valence-band dispersion relations for the A line of silver from the adjusted bands in Fig. 3. They are set out in Table I. While the adjustment gave a visually dramatic improvement, the actual adjustment of the bands was in fact very small, rarely exceeding 0.2 eV and in most places being essentially nil. The only adjustment that is easily apparent by inspection is the distance between bands 4 and 6 where they



appear to be repelling, about halfway between  $\Gamma$  and L. We find these bands about 0.9 eV apart at this point, while they approach one another to within about 0.6 eV in Christensen's RAPW band structure.<sup>15</sup> With this exception, the agreement between this theoretical band structure and experiment is excellent.

Because our results provide the first measurement of the silver d-band energies at  $\Gamma$ , where the crystal momentum is zero and ligand-field concepts are applicable, it is interesting to note the relative strengths of the crystal field and the spin-orbit coupling at  $\Gamma$ . The appropriate crystal-field Hamiltonian<sup>3</sup> has the form

$$\mathcal{H} = A_4 T_4 + \xi \vec{l} \cdot \vec{s}$$

where  $A_4$  is the crystal field strength.  $T_4$  is a suitable linear combination of spherical harmonics  $Y_{4m}$ , and  $\xi$  is the spin-orbit coupling constant. In a  $d^1$  (or  $d^9$ ) manifold,  $\mathcal{H}$  has three irreducible representations:

$$\mathcal{H} \rightarrow 2\Gamma_8 + \Gamma_7$$

The  $\Gamma_8$  representations have twofold orbital degeneracy, while  $\Gamma_7$  is singly degenerate. Taking  $10Dq$  as the energy spacing due to the  $A_4 T_4$  term alone, the energy levels lie at<sup>21</sup>

$$E(\Gamma_8) = -4Dq - \frac{1}{2}\xi - \frac{\sqrt{3}}{2}\xi \cot \theta$$

$$E(\Gamma_7) = -4Dq + \xi$$

$$E(\Gamma_8) = 6Dq + \frac{\sqrt{3}}{2}\xi \cot \theta \quad ,$$

where  $\theta$  is defined by

$$\tan 2\theta = \frac{-\sqrt{6} \xi}{10Dq + \xi/2}$$

The relative spacing of the three levels, 0.39:0.61, as determined from this experiment, is only consistent with the above equations for any values of  $10Dq$  and  $\xi$  if  $\Gamma_7$  lies between the two  $\Gamma_8$  levels. This is consistent with Christensen's band structure. There are still two regions with this relative spacing and the level order  $\Gamma_8\Gamma_7\Gamma_8$  (Fig. 4). With no knowledge of the sign or magnitude of  $\xi$  or  $10Dq$ , we could not decide between the two. However, by using only the fact that the  $\Gamma_7$  level lies closer to the lower  $\Gamma_8$  level, together with the expected sign  $\xi > 0$  for an electron,<sup>22</sup> we can unambiguously select region B in Fig. 4. Solving for the two parameters, we find

$$10Dq = 0.85 \pm 0.03 \text{ eV}$$

$$\xi = 0.24 \pm 0.01 \text{ eV}$$

We have used the spacings  $\Delta E(\Gamma_8-\Gamma_8) = 1.13 \text{ eV}$ ,  $\Delta E(\Gamma_7-\Gamma_8) = 0.44 \text{ eV}$ , derived from the energies in Table I. It is gratifying that the derived value of  $\xi(4d)$  lies within 7% of the free-atom value (0.224 eV).<sup>3</sup> Because  $\xi(4d)$  is expected to change very little between the free atom and the solid,<sup>23</sup> an arguably equally valid alternative procedure would be to force-fit the experimental energies with  $\xi(4d)$  constrained to the free-atom

value. This approach yields

$$10Dq = 0.88 \text{ eV, for}$$

$$\xi(4d) = 0.224 \text{ eV.}$$

Taking into account both the intrinsic experimental errors and the range of values allowed by these two analyses, our final values are

$$10Dq = 0.865 \pm 0.027 \text{ eV}$$

$$\xi(4d) = 0.232 \pm 0.011 \text{ eV}$$

for silver metal. It is interesting to note that the positive sign of  $10Dq$  for (face-centered cubic) silver represents an attractive interaction of the  $d$  electrons with the nearest neighbor at  $\Gamma$  (the  $t_{2g}$  levels are favored).

Although the above ligand field analysis yielded results in excellent agreement with Christensen's band structure, it was based entirely on our experimental energies.

#### IV. TWO UNUSUAL EFFECTS IN ARP FROM Ag(111)

In this Section we discuss briefly two unexpected effects that arose during this study. Both are attributed to the structure of the conduction bands, and both may be expected to arise in other angle-resolved photoemission studies.

A. The  $\Gamma_7$ - $\Gamma_8$  Resonance at  $h\nu = 22$  eV

Near  $\Gamma$  the d bands of silver are flat and fall into the  $\Gamma_8\Gamma_7\Gamma_8$  levels, as discussed above. For photon energies of 24 eV and above the two  $\Gamma_8$  peaks dominate the spectrum (Fig. 1), while the  $\Gamma_7$  peak is not evident. At photon energies of  $h\nu = 20$  eV and below the four bands formed by splitting of the two  $\Gamma_8$  bands are nearly always resolved. The  $\Gamma_7$  band, which (theoretically) remains essentially flat along  $\Lambda$  to the L point, is not evident in the spectra for photon energies below 20 eV or above 24 eV. At  $h\nu = 22$  eV, however, it yields the highest feature in the spectrum, as a third peak between the two  $\Gamma_8$ -derived features. At  $h\nu = 21.2$  eV it also appears, better resolved<sup>12</sup> but less intense, in the same position. By curve-fitting we established this feature as present, but weak, in the spectra at  $h\nu = 20$  and 24 eV. Thus the  $\Gamma_7$  peak intensity appears to be resonant around  $h\nu = 22$  eV. We attribute this behavior to the final-state band labeled  $6^-$  in Christensen's band structure (Fig. 5), which becomes flat over a sizeable fraction ( $\sim 0.2$ ) of the  $\Lambda$  line near  $\Gamma$ , and lies at 22 eV above  $\Gamma_7$ . The probability of photoemission along [111] appears to be resonantly enhanced by the very large joint density of states afforded by the flat initial- and final-state bands ( $\Gamma_7$  and  $\Gamma_6$ , respectively) at  $h\nu = 22$  eV. A similar effect would be expected in ARP spectra from gold along [111] in the photon energy range  $h\nu = 16$ -22 eV, because the conduction bands are calculated to be similar to those of silver and the valence bands are also flat near  $\Gamma$ .<sup>24</sup>

### B. The 17-eV Kinetic Energy Peak

For photon energies of  $h\nu = 26$  eV and above, our spectra show an additional weak feature which falls at  $\sim 17.5$  eV kinetic energy relative to  $E_F$ , independent of photon energy. This feature is about 1 eV wide, but its low intensity and the presence of inelastic background inhibit an accurate determination of its width and shape. We attribute this feature to conduction electrons that have been excited to higher energies, then inelastically scattered and trapped in band 7 and perhaps band 8 (see Fig. 5). These bands lie at about 17 eV above  $E_F$ , as discussed above for band 7 ( $\Gamma_6$ ), are quite flat, and should contain a significant amount of plane-wave character with a [111] propagation direction. Thus these bands possess all the attributes of a high probability of being occupied (and no unoccupied bands below them for electrons to scatter into) and the correct crystal momentum and energy to be observed in this experiment. Furthermore, we can think of no other mechanism leading to a constant kinetic energy peak at 17 eV.

This particular effect appears to be new in angle-resolved photoemission, but the idea of structure in the inelastic tails of photoemission spectra due to conduction-band density-of-states (DOS) effects is well-known. Energetic electrons must move through the lattice in conduction-band states, and the "true" inelastic tail from the sample (as opposed to contributions from scattering on the analyzer grids) must be related to the conduction band structure. Of course, angle-averaging,

coupled to the relatively featureless shape of the typical conduction-band DOS, preclude observation of significant structure in most cases. For Ag(111) the angle-resolved nature of this experiment, together with the unusual character of band 7, combine to produce a peak strong enough to be noticed accidentally.

In a broader context this effect is simply a new manifestation of angle-resolved secondary electron emission (ARSEE), which has been studied in detail by Willis and co-workers.<sup>25</sup> In fact our experiment differs from theirs only in the excitation mechanism, using photoelectrons rather than high-energy electrons. If the experimental conditions were carefully adjusted, photon-stimulated ARSEE might be made to provide conduction-band information complementary to that obtained from constant initial state photoemission or from electron-induced ARSEE.

ACKNOWLEDGEMENTS

This work was performed at the Stanford Synchrotron Radiation Laboratory, which is supported by the NSF Grant No. DMR 73-07692 A02, in cooperation with the Stanford Linear Accelerator Center and was done with support from the Division of Chemical Sciences, Office of Basic Energy Sciences, U. S. Department of Energy.

Table I. Derived Valence-Band Energies for Silver Along  $\Lambda$  (in eV).<sup>a</sup>

$k/(\frac{\pi}{4a})$	band 1	band 2	band 3	band 4	band 5	band 6
000( $\Gamma$ )	(7.44)	5.92	5.92	5.48	4.78	4.78
	— <sup>b</sup>	.02	.02	.02	.03	.03
111	7.05	5.89	5.85	5.39	4.74	4.72
	—	.00	.00	.00	-.07	-.01
222	6.62	5.81	(5.30)	5.11	4.62	4.16
	—	-.01	(.01)	.06	-.04	-.37
333	(6.84)	5.80	(5.45)	4.55	4.27	2.33
	—	-.13	(.00)	.14	.11	-.09
444(L)	(6.94)	(5.82)	(5.53)	(4.20)	(3.96)	0.30
	—	(-.17)	(.00)	(.00)	(-.01)	.14

- a) Binding energies relative to  $E_F$  are given, with deviations of these numbers from those in Christensen's RAPW calculation give below. Parentheses mean that no data were available at these points.
- b) Band 1 was not adjusted. The sparse data fit the RAPW curve very well.



REFERENCES

1. K. Siegbahn, et al., ESCA - Atomic Molecular and Solid-State Structure by Means of Electron Spectroscopy, Nova Acta R. Soc. Sci. Ups. Ser. IV, 20 75 (1967).
2. C. S. Fadley and D. A. Shirley, J. Research Nat. Bur. Std. A, Phys. and Chem., 74A, 543 (1970).
3. L. Ley, S. P. Kowalczyk, F. R. McFeely, and D. A. Shirley, Phys. Rev. B10, 4881 (1974).
4. R. A. Pollak, L. Ley, S. P. Kowalczyk, and D. A. Shirley, Phys. Rev. Lett. 29, 274 (1972).
5. N. V. Smith, G. K. Wertheim, S. Hüfner, and M. M. Traum, Phys. Rev. B10, 3197 (1974).
6. C. N. Berglund and W. F. Spicer, Phys. Rev. 136, A1030 (1964); ibid, p. A1044.
7. L. Walldén and T. G. Gustafsson, Phys. Scr. 6, 73 (1972).
8. P. O. Nilsson and D. E. Eastman, Phys. Scr. 8, 113 (1973).
9. N. V. Smith and M. M. Traum, Phys. Rev. Lett. 29, 1243 (1972).
10. T. Gustafsson, P. O. Nilsson, and L. Walldén, Phys. Lett. A 37, 121 (1971).
11. H. Becker, E. Dietz, U. Gerhardt, and H. Angermüller, Phys. Rev. B12, 2084 (1975).
12. H. F. Roloff and H. Neddermeyer, Solid State Commun. 21, 561 (1977).
13. G. V. Hansson and S. A. Flodström, Phys. Rev. B17, 473 (1978).

14. D. Liebowitz and N. J. Shevchik, Phys. Rev. B17, 3825 (1978).
15. N. E. Christensen, Phys. Status Solids B 54, 551 (1972).
16. D. A. Shirley, J. Stöhr, P. S. Wehner, R. S. Williams, and G. Apai, Physica Scripta 16, 398 (1977); J. Stöhr, P. S. Wehner, R. S. Williams, and D. A. Shirley, Phys. Rev. B17, 587 (1978).
17. J. Stöhr, G. Apai, P. S. Wehner, F. R. McFeely, R. S. Williams, and D. A. Shirley, Phys. Rev. B14, 5144 (1976).
18. P. S. Wehner, "Valence Band Photoemission Studies of Clean Metals", April, 1978 (Ph.D. Thesis, University of California, Berkeley; Lawrence Berkeley Laboratory Report LBL-7622).
19. N. J. Shevchik, J. Phys. C, L555 (1977); N. J. Shevchik, Phys. Rev. B16, 3428 (1977); R. S. Williams, P. S. Wehner, J. Stöhr, and D. A. Shirley, Phys. Rev. Lett. 39, 302 (1977).
20. R. C. Jaklevic and John Lambe, Phys. Rev. B12, 4146 (1975).
21. For a good discussion of the specific problem of a d electron in a cubic field, with spin-orbit splitting, see Carl J. Ballhausen, Introduction to Ligand Field Theory (McGraw-Hill, 1962), p. 118.
22. The signs would of course be reversed for a  $d^9$  final (hole) state.
23. Indeed, even a 7% variation in  $\xi$  is probably too large, because  $\xi$  is determined mainly by properties of the ion core. See Ref. 3.

24. N. E. Christensen, Phys. Rev. B13, 2698 (1976).
25. R. F. Willis, B. Feuerbacher, and N. E. Christensen, Phys. Rev. Lett. 38, 1075 (1977); R. F. Willis and N. E. Christensen, Paper IIIi, to be published in the proceedings of VUV-5, the Fifth International Conference on Vacuum Ultraviolet Physics, Montpellier, France, September 5-9, 1977.

FIGURE CAPTIONS

- Figure 1. Electron energy distributions at normal emission for Ag(111) in the range  $h\nu = 6$  to 32 eV. The region of predominantly sp emission near  $E_F$  is magnified for most spectra. For  $h\nu = 26$  to 32 eV the region containing the constant final state feature is also magnified.
- Figure 2. Valence-band energies of silver along  $\Lambda$ , versus the k-point along  $\Lambda$  in the second zone that corresponds to each photoemission peak. A partial photon energy scale is indicated along the top, together with dashed curves for the conduction band (band 7) displaced down by 6 eV and by 10 eV. Christensen's band structure is plotted, together with our data (open circles) and those of Hansson and Flodström (filled circles from 7 eV to 11.6 eV), Roloff and Neddermeyer (filled circles at 11.83, 16.85, and 21.22 eV), and Liebowitz and Shevchik (filled circles at 26.9 and 40.8 eV).
- Figure 3. Valence-band energies of silver along  $\Lambda$  after adjustment. The binding energies of Hansson and Flodström's data were increased by 0.18 eV and those of Roloff and Neddermeyer were reduced by 0.25 eV, bringing the experimental points into very good agreement. Christensen's bands were then adjusted to fit the data, with the additional constraint that band 6 lie

0.3 eV below  $E_F$ , as required by the tunnelling results of Jaklevic and Lambe. Derived energies are set out in Table I.

Figure 4. Energies of the three irreducible representations of a d electron in a cubic field, and with spin-orbit splitting, as functions of the ratio  $10Dq/(5/2)\xi$ . A and B are the only two regions in which the level splittings have ratios near 3:2, as in silver, for any values of  $10Dq/(5/2)\xi$ . Region B applies to silver.

Figure 5. The Ag band structure along  $\Lambda$  as calculated in Ref. 15.

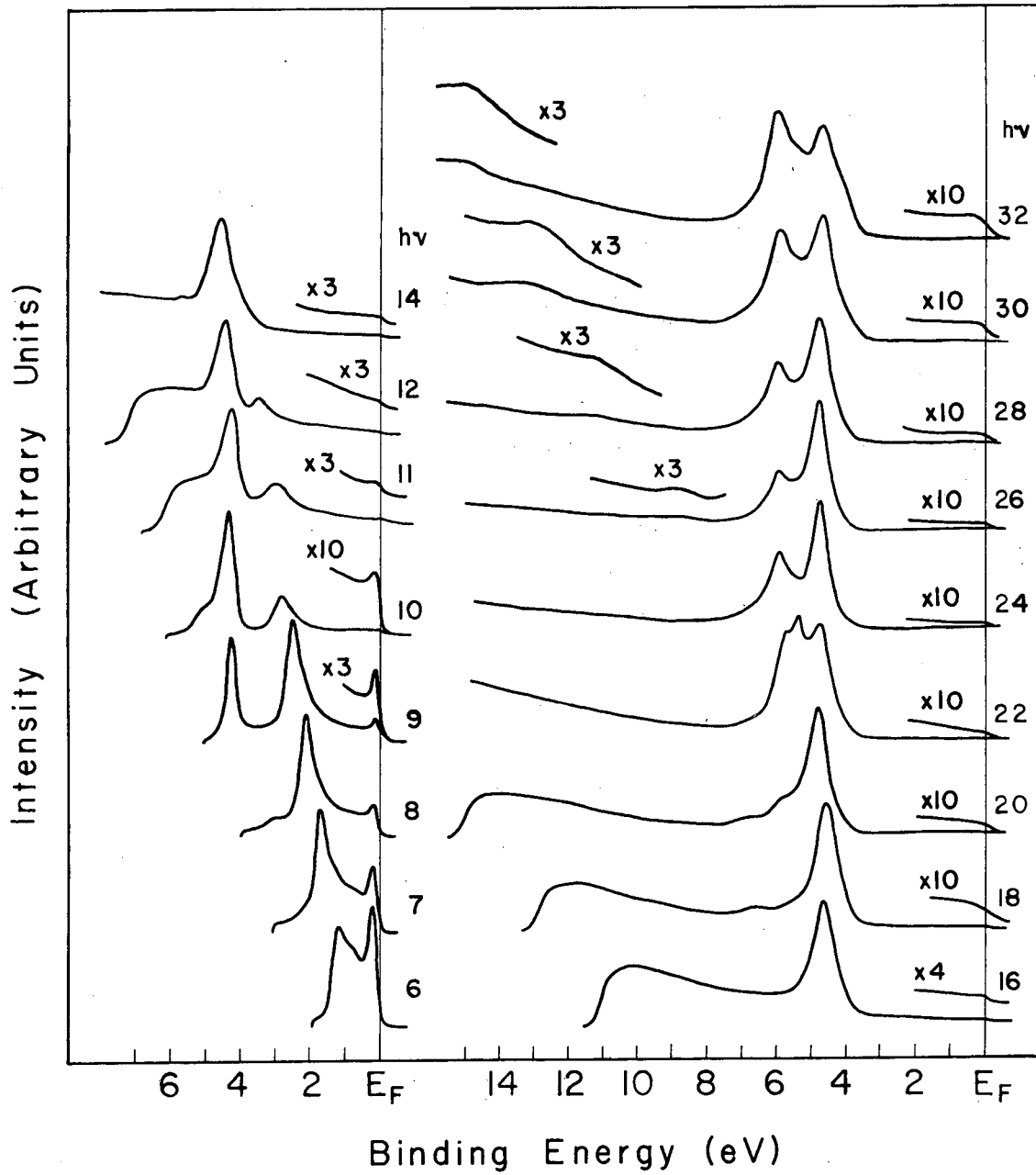
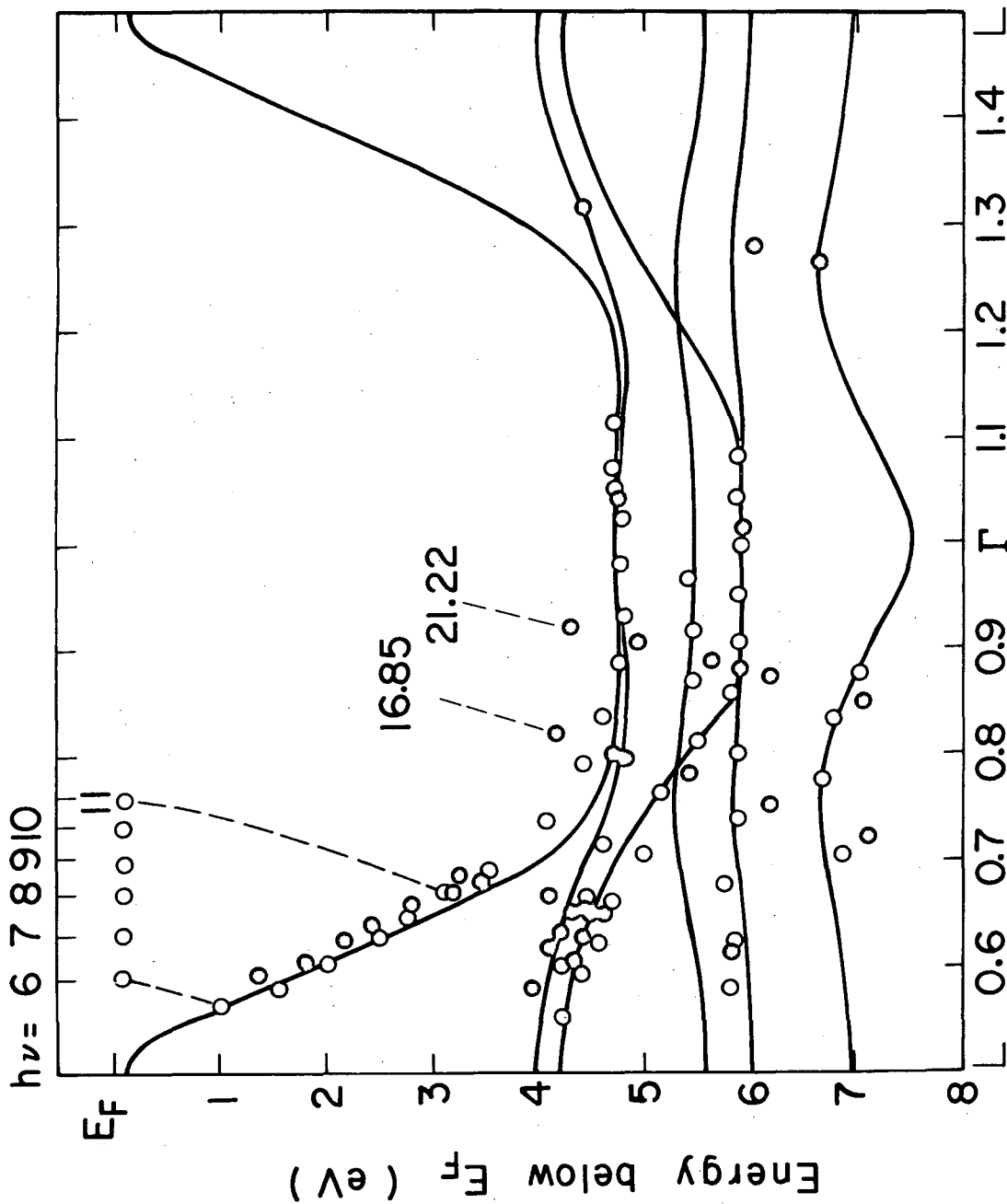


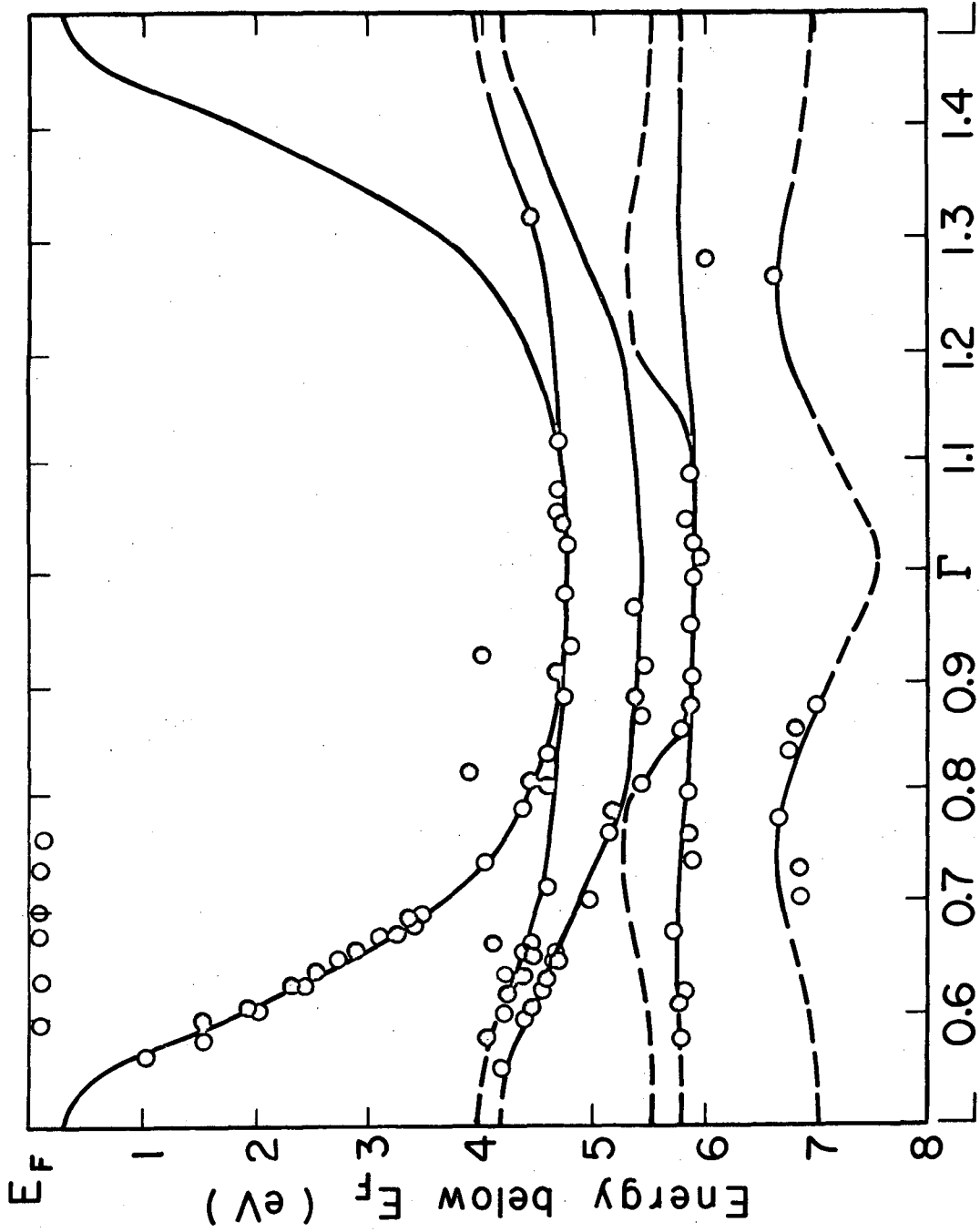
Figure 1

XBL 7810-11893



XBL 789 - 22.73

Figure 2

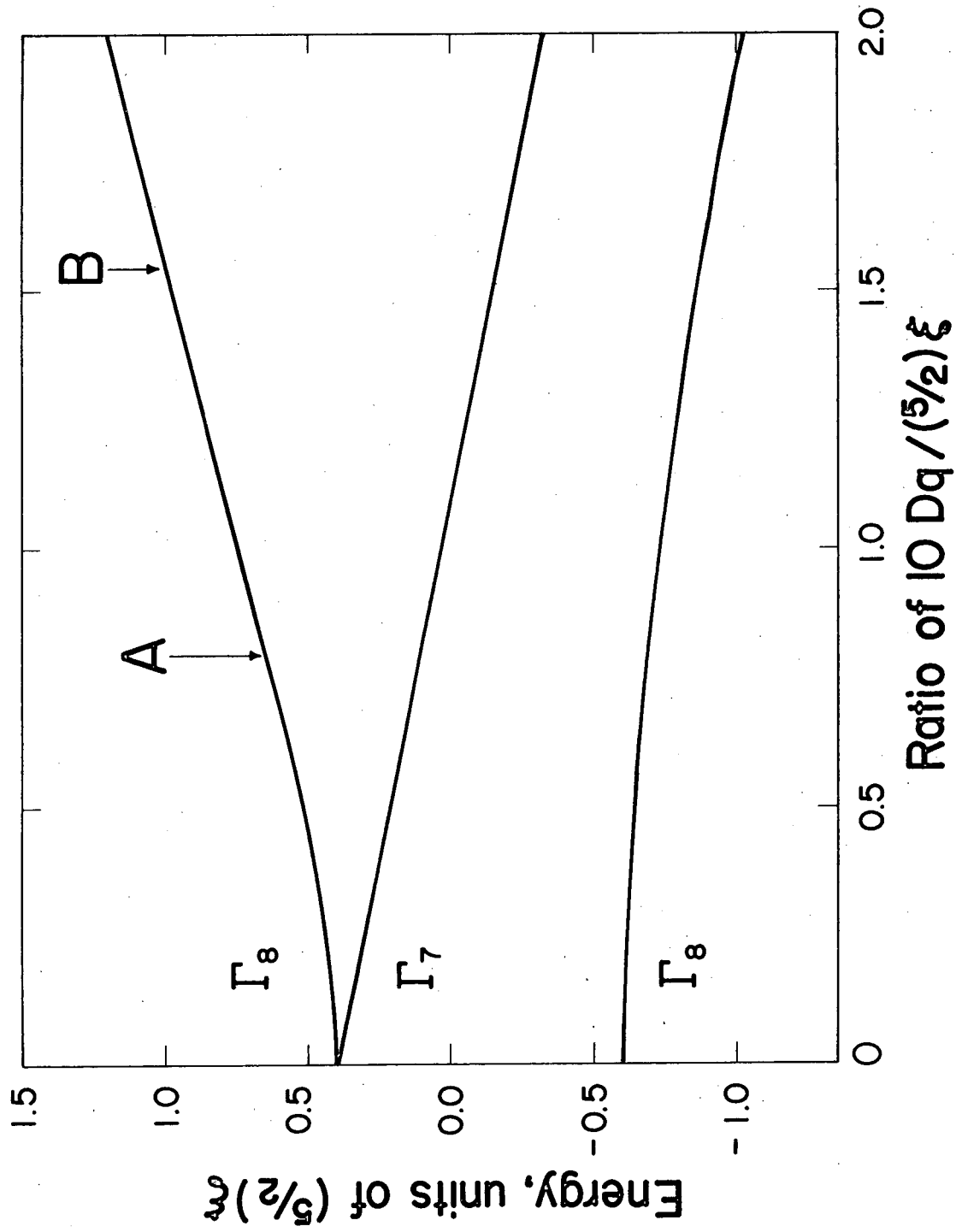


Final-state crystal momentum along  $\Delta$

XBL789 - 2274

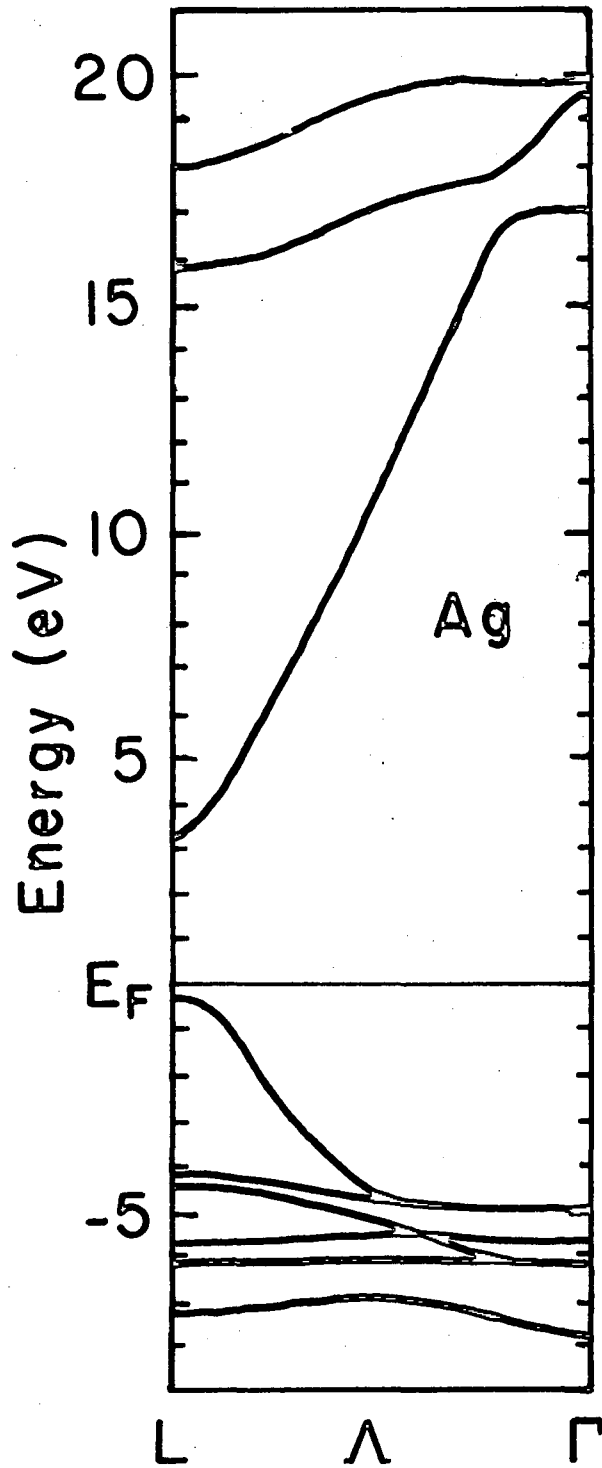
Figure 3





XBL 789 - 2272

Figure 4



XBL 7810-11892

Figure 5

This report was done with support from the Department of Energy. Any conclusions or opinions expressed in this report represent solely those of the author(s) and not necessarily those of The Regents of the University of California, the Lawrence Berkeley Laboratory or the Department of Energy.

TECHNICAL INFORMATION DEPARTMENT  
LAWRENCE BERKELEY LABORATORY  
UNIVERSITY OF CALIFORNIA  
BERKELEY, CALIFORNIA 94720